

Memory-Efficient 4-bit Preconditioned Stochastic Optimization

Jingyang Li¹

Kuangyu Ding¹

Kim-Chuan Toh¹

Pan Zhou²

¹ National University of Singapore

² Singapore Management University

¹{li-jingyang, kuangyud}@u.nus.edu mattohkc@nus.edu.sg

²panzhou@smu.edu.sg

Abstract

Preconditioned stochastic optimization algorithms, exemplified by Shampoo, have demonstrated superior performance over first-order optimizers, providing both theoretical advantages in convergence rates and practical improvements in large-scale neural network training. However, they incur substantial memory overhead due to the storage demands of non-diagonal preconditioning matrices. To address this, we introduce 4-bit quantization for Shampoo’s preconditioners. We introduced two key methods: First, we apply Cholesky decomposition followed by quantization of the Cholesky factors, reducing memory usage by leveraging their lower triangular structure while preserving symmetry and positive definiteness to minimize information loss. To our knowledge, this is the first quantization approach applied to Cholesky factors of preconditioners. Second, we incorporate error feedback in the quantization process, efficiently storing Cholesky factors and error states in the lower and upper triangular parts of the same matrix. Through extensive experiments, we demonstrate that combining Cholesky quantization with error feedback enhances memory efficiency and algorithm performance in large-scale deep-learning tasks. Theoretically, we also provide convergence proofs for quantized Shampoo under both smooth and non-smooth stochastic optimization settings.

1. Introduction

Deep learning has achieved significant advancements across numerous fields in recent years, including language modeling [7, 46], computer vision [16], and multi-modality [37]. These advancements are primarily driven by the scaling of model size, dataset volume, and computational power, as outlined in scaling laws that demonstrate the impact of increased resources on model performance [24, 25]. This trend of scaling has further extended into specialized domains such as finance [51], material science [52], and healthcare [30].

Along with the size growth of large-scale models, stochastic gradient descent (SGD) has become a widely adopted method for training thanks to its efficiency and

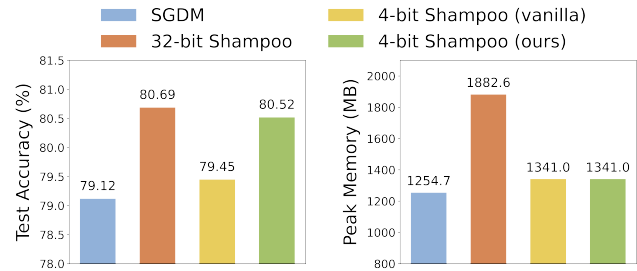


Figure 1. Comparison of test accuracy and peak memory usage for training ResNet-34 on CIFAR-100 dataset.

simplicity [23, 39, 43]. However, adaptive gradient methods, e.g., Adagrad [17], Adam [26], and AdamW [34], apply a diagonal preconditioning to the gradient, which enables faster convergence than SGD [17, 59]. These adaptive methods have demonstrated empirical advantages in various applications [16, 54] and are now the standard optimizers for training large-scale neural networks.

Building on adaptive gradient methods, full-matrix preconditioned gradient methods offer theoretically superior convergence by capturing richer correlations among parameters [17]. Despite these theoretical advantages, however, the memory overhead associated with non-diagonal matrices poses a significant challenge for large-scale neural networks, which can contain millions of parameters [16, 23, 33]. To address this, a range of efficient preconditioned gradient methods, such as K-FAC [35], Shampoo [22], K-BFGS [20], and AdaBK [56], aim to make full-matrix preconditioning computationally feasible by approximating the full-matrix precondition, e.g., block-diagonal precondition matrix. These algorithms have shown faster convergence rates in practice when compared to both SGD and adaptive gradient methods [3, 41, 56].

Nevertheless, these efficient preconditioned methods still impose substantial memory costs that restrict their scalability in practical and large-scale model applications. As shown in Fig. 1, the peak memory usage of methods like Shampoo remains significantly higher than SGD. While quantizing precondition matrices in these preconditioned methods from high-precision to low-precision, e.g., 32-bit to 4-bit, effectively reduces memory usage, it

also inevitably introduces information loss, which, in turn, severely degrades the performance of these preconditioned methods. This is validated by Fig. 1: compared with 32-bit Shampoo, 4-bit Shampoo enjoys much less memory cost but suffers from much worse performance. Therefore, for these efficient preconditioned methods, carefully designed strategies are essential to effectively compress precondition matrices without compromising optimization quality.

Contribution. In this work, we are particularly interested in Shampoo because of its simplicity, effectiveness and also popularity, and aim to enable effective 4-bit quantization of preconditioners while preserving the stability and efficiency of preconditioned gradient methods. Our main contributions are highlighted below.

Firstly, we introduce Cholesky quantization to improve memory efficiency and stability of 4-bit quantization. Instead of quantizing the preconditioners directly, we first apply Cholesky decomposition on the precondition matrices, and then quantize their corresponding Cholesky factors. This approach not only reduces storage requirements—Cholesky factors occupy roughly half the space of the original precondition matrices—but also retains symmetry and positive definiteness in the decomposed matrices, mitigating quantization-induced information loss. Our approach leverages these intrinsic matrix properties without adding significant computational overhead, marking the first known application of quantization to Cholesky factors for preconditioned gradient descent.

Secondly, we introduce an error feedback strategy for Cholesky quantization to further reduce its quantization information loss. Inspired by prior works in distributed training with low-precision communication [40, 44, 53], we maintain a 4-bit error state, which exponentially-moving averages all historical quantization errors of a Cholesky factor for stable error estimation. Then, this error state is used to compensate the corresponding Cholesky factor to cancel its potential quantization error at current quantization iteration, thereby achieving more lossless quantization. Moreover, as Cholesky factor and its error state are triangular, they can be stored together in a matrix, saving memory cost.

Thirdly, we establish convergence results for quantized Shampoo in both smooth and nonsmooth stochastic non-convex optimization settings. In smooth case, our 4-bit Shampoo achieves optimal convergence rate of $\mathcal{O}(\frac{1}{\sqrt{T}})$. Additionally, we are the first to prove global convergence for preconditioned gradient descent in the nonsmooth non-convex setting, which applies to scenarios with nonsmooth activation functions, such as ReLU in ResNet [23]. Under mild conditions, we show the sequence converges to stationary points set of the nonsmooth nonconvex problem.

Finally, we apply the above techniques to quantize Shampoo into our 4-bit Shampoo, and evaluate it on representative image classification tasks using both convolutional

neural networks (CNNs) and vision transformers (ViTs). Across these benchmarks, our 4-bit Shampoo significantly surpasses vanilla 4-bit Shampoo in performance. Compared with vanilla 32-bit Shampoo, our 4-bit Shampoo significantly reduces memory usage while achieving comparable test performance, enabling larger models to be trained within existing computational resource limits.

2. Related Work

Preconditioned Stochastic Optimization. Adaptive gradient methods are the most widely used preconditioned gradient methods in training neural networks, with Adagrad [17], RMSProp [45], and Adam [26] being notable examples. They use diagonal preconditioners to rescale the gradients, been shown to improve convergence in stochastic settings. Preconditioned gradient methods with non-diagonal preconditioners offer faster convergence in theory [17], and are widely explored recently due to faster convergence than adaptive gradient methods in practice [20, 22, 35, 56]. Among them, Shampoo [22] receives extensive concern for its simplicity and effectiveness [36, 48], and it has been developed for large-scale distributed training [3, 41].

Quantization for Optimizers. Quantization has been widely used for gradient compression to enable efficient communication in large-scale optimization, particularly for distributed training [2, 47, 49]. Recent works have extended quantization to optimizer states—such as the momentum or second-moment estimates used by adaptive optimizers like Adam—to decrease peak memory usage during neural network training [15, 32]. Despite its computational efficiency, quantization incurs information loss, which can degrade algorithmic performance. To address this, ongoing research explores techniques such as error feedback compensation to mitigate these effects and improve robustness [38, 40].

3. Preliminaries

Here we introduce practical Shampoo from [22] and linear-square (linear-2) quantization [15] to compress the preconditioning matrices in our algorithm.

Notations. Let $\|A\|_F = \sum_{ij} A_{ij}^2$ denote the Frobenius norm of a matrix A . $A \otimes B$ means the Kronecker product of A and B . For a symmetric matrix H , $\lambda_{\max}(H)$ and $\lambda_{\min}(H)$ denote the maximum and minimum eigenvalues of H , respectively. For square symmetric matrices A and B , we write $A \preceq B$ if $B - A$ is positive semidefinite (PSD). Quantization and dequantization operations are denoted by \mathcal{Q} and \mathcal{D} , respectively.

3.1. Practical Shampoo

When minimizing a nonconvex stochastic objective function

$$F(W) := \mathbb{E}_{\xi \sim \Xi} [F(W, \xi)], \quad (1)$$

where $W \in \mathbb{R}^{m \times n}$ is the parameter of the learning model, and data ξ is drawn from an unknown distribution Ξ . At each iteration, we sample a mini-batch of data points to

compute the stochastic gradient $G \in \mathbb{R}^{m \times n}$, and use this stochastic gradient to update the model parameter W .

To accelerate convergence, Shampoo preconditiones the stochastic gradient used in first-order optimizers. Specifically, at iteration k , it updates the preconditioning states L_k and R_k with stochastic gradient G_k for preconditioning:

$$\begin{cases} L_k = \beta L_{k-1} + (1 - \beta) G_k G_k^T, \\ R_k = \beta R_{k-1} + (1 - \beta) G_k^T G_k, \\ \hat{G}_k = L_k^{-1/4} G_k R_k^{-1/4}, \end{cases} \quad (2)$$

where $\beta \in (0, 1)$, and the $1/4$ -th root inverse is computed efficiently using the Schur-Newton algorithm [21].

Next, first-order base optimizer \mathcal{F} like SGD can use the preconditioned gradient \hat{G}_k in Eq. (2) to replace vanilla G_k for model update. For efficiency, Shampoo stores $(L_k, R_k, L_k^{-1/4}, R_k^{-1/4})$, and updates (L_k, R_k) for every T_1 iterations and $(L_k^{-1/4}, R_k^{-1/4})$ every T_2 iterations. See practical Shampoo algorithm in Algorithm 2 of Appendix A.

3.2. Linear Square Quantization for Compression

Quantization compresses tensors from high precision floating-point to low precision, reducing memory usage. Following [15, 32], we use block-wise quantization to mitigate outlier effects. Below, we introduce the quantization and dequantization processes, focusing on the two-dimensional tensor (matrix) case of Shampoo.

Quantization. For a floating-point matrix $X \in \mathbb{R}^{m \times n}$, we partition it into blocks of size $B \times B$, resulting in $P = \lceil m/B \rceil \times \lceil n/B \rceil$ blocks $\{X_p\}_{p=1}^P$. In each block X_p , a normalization factor $N_p = \max\{|X_p|\}$ scales elements to $[-1, 1]$ via $\bar{X}_p = X_p/N_p$. Each element \bar{x}_p in \bar{X}_p is then quantized to a b -bit integer using a quantization mapping $\mathcal{M} : [0, 2^b - 1] \cap \mathbb{Z} \rightarrow [-1, 1]$, calculated by:

$$q_p = \arg \min_{j \in [0, 2^b - 1] \cap \mathbb{Z}} |\bar{x}_p - \mathcal{M}(j)|.$$

Common quantization mappings include linear, dynamic, and quantile mappings [15, 32]. Here we use a linear-2 mapping for simplicity and efficiency when $b = 4$:

$$\mathcal{M}(j) = \begin{cases} -(-1 + \frac{2j}{2^b-1})^2, & j < 2^{b-1} - 1, \\ 0, & j = 2^{b-1} - 1, \\ (-1 + \frac{2j}{2^b-1})^2, & j > 2^{b-1} - 1, \end{cases}$$

where $j \in \{0, 1, \dots, 2^b - 1\}$. This block-wise quantization can be efficiently executed in parallel on GPUs [19, 55].

Dequantization. Dequantization \mathcal{D} reverses the quantization process. For each quantized block Q_p , we map each element q_p back to $[-1, 1]$ via $\bar{x}'_p = \mathcal{M}(q_p)$ to obtain \bar{X}'_p . We then restore the original scale using N_p , giving $X'_p = \mathcal{D}(Q_p) = N_p \bar{X}'_p$. Like quantization, dequantization is parallelizable on GPUs.

For block size $B \times B$, it balances accuracy and memory cost: smaller blocks improve accuracy but increase the number of normalization factors, raising memory overhead.

4. Memory-Efficient Shampoo Via Compensated Cholesky Quantization

We begin by detailing a direct quantization-based compression method to reduce the memory overhead caused by Shampoo’s preconditioning matrices in Sec. 4.1. Next, in Sec. 4.2, we introduce a more memory-efficient Cholesky quantization approach to improve upon the vanilla quantization in Sec. 4.1. Finally, in Sec. 4.3, we design a compensation strategy to mitigate information loss introduced by Cholesky quantization.

4.1. Quantization for Shampoo Compression

From Sec. 3.1, one knows that Shampoo requires storage of four preconditioning matrices $(L_k, R_k, L_k^{-1/4}, R_k^{-1/4})$, each sized $d \times d$, where d denotes the model parameter dimension. This brings much additional GPU memory cost, and becomes even more pronounced when training modern neural networks, which are often extremely high-dimensional. So reducing Shampoo’s memory overhead is essential for efficient and scalable network training.

A straightforward approach is to use a quantizer \mathcal{Q} , e.g., the linear-2 quantization in Sec. 3.2, to compress the preconditioners in Shampoo for saving memory, and then adopt a dequantizer \mathcal{D} to recover them for subsequent usage. Formally, at iteration k , we can compute two low-precision preconditioning states (\bar{L}_k, \bar{R}_k) as

$$\begin{aligned} L_k &= \beta \mathcal{D}(\bar{L}_{k-1}) + (1 - \beta) G_k G_k^T, \quad \bar{L}_k = \mathcal{Q}(L_k), \\ R_k &= \beta \mathcal{D}(\bar{R}_{k-1}) + (1 - \beta) G_k^T G_k, \quad \bar{R}_k = \mathcal{Q}(R_k). \end{aligned} \quad (3)$$

In this work, we use 4-bit precision for efficient storage. For $\bar{L}_k^{-1/4}, \bar{R}_k^{-1/4}$, we update them as

$$\begin{aligned} L_k &= \mathcal{D}(\bar{L}_k), \quad \bar{L}_k^{-1/4} = \mathcal{Q}((L_k + \lambda_{\max}^L \epsilon I_m)^{-1/4}), \\ R_k &= \mathcal{D}(\bar{R}_k), \quad \bar{R}_k^{-1/4} = \mathcal{Q}((R_k + \lambda_{\max}^R \epsilon I_n)^{-1/4}), \end{aligned} \quad (4)$$

where, same as vanilla Shampoo, $\lambda_{\max}^L \epsilon I_m$ and $\lambda_{\max}^R \epsilon I_n$ provide numerical stability during the Schur-Newton iterations used to calculate the inverse $1/4$ -th roots, in which $\lambda_{\max}^L, \lambda_{\max}^R$ are the maximal singular values of L_k, R_k , and ϵ is a small constant [56].

Accordingly, one can store 4-bit $(\bar{L}_k, \bar{R}_k, \bar{L}_k^{-1/4}, \bar{R}_k^{-1/4})$ instead of their original 32-bit versions, and dequantize them for usage, e.g., dequantizing $(\bar{L}_k^{-1/4}, \bar{R}_k^{-1/4})$ to compute preconditioned gradient in Eq. (2).

Despite its simplicity, direct quantization of preconditioners as in Eq. (3) and Eq. (4) can lead to performance degradation due to information loss, e.g., quantizing them from 32-bit to 4-bit precision. For instance, when training ViT-Small [16] on CIFAR-100 [27] with Shampoo using AdamW as the base optimizer, the 32-bit version Shampoo achieves 78.21% test accuracy, substantially outperforming the 4-bit quantized Shampoo, which reaches only 74.56%. Further experimental comparisons can be found in Section 6.

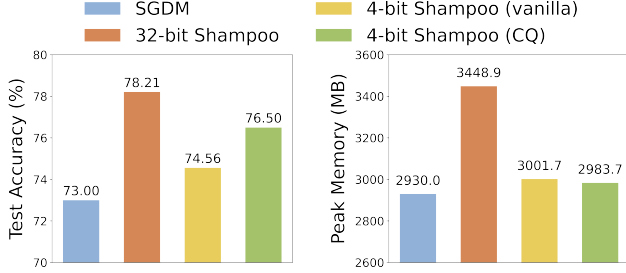


Figure 2. Comparison of test accuracy (%) and peak memory usage (MB) with ViT-Small on CIFAR-100 for vanilla 4-bit Shampoo and 4-bit Shampoo with Cholesky quantization (CQ).

4.2. Efficient and Stable Cholesky Quantization

Here we introduce Cholesky quantization to further improve memory efficiency and also stability of quantization in Sec. 4.1. Instead of quantizing L_k and R_k , we apply Cholesky decomposition on L_k and R_k , and quantize their corresponding Cholesky factors as \bar{C}_k^L and \bar{C}_k^R which are two lower triangular matrices and require much less storage. Formally, at iteration k , this process can be written as

$$\begin{aligned}
 L_{k-1} &= \mathcal{D}(\bar{C}_{k-1}^L) \mathcal{D}(\bar{C}_{k-1}^L)^T, R_{k-1} = \mathcal{D}(\bar{C}_{k-1}^R) \mathcal{D}(\bar{C}_{k-1}^R)^T, \\
 L_k &= \beta L_{k-1} + (1-\beta) G_k G_k^T, R_k = \beta R_{k-1} + (1-\beta) G_k^T G_k, \\
 C_k^L &= \text{Cholesky}(L_k + \epsilon I), C_k^R = \text{Cholesky}(R_k + \epsilon I),
 \end{aligned} \tag{5}$$

where $\text{Cholesky}(L_k + \epsilon I)$ computes a lower triangular matrix C_k^L such that $C_k^L C_k^{L^T} = L_k + \epsilon I$. The small term ϵI is added for numerical stability, with ϵ as small constant. Once C_k^L and C_k^R are computed, they are quantized as:

$$\bar{C}_k^L = \mathcal{Q}(C_k^L), \quad \bar{C}_k^R = \mathcal{Q}(C_k^R). \tag{6}$$

Accordingly, we can only store two quantized lower triangular matrices \bar{C}_k^L and \bar{C}_k^R . Here we quantize the non-diagonal part of \bar{C}_k^L and \bar{C}_k^R into 4-bit precision while retaining the diagonal elements for 32-bit. This approach is used because non-diagonal elements have less impact on numerical stability, allowing reduced precision with minimal accuracy loss. In contrast, diagonal elements are crucial for overall stability and accuracy, so keeping them in 32-bit helps prevent error accumulation in the factorization.

Now we discuss two advantages of Cholesky quantization. Firstly, Cholesky factors are lower triangular matrices and their maintaining only need nearly half of the GPU memory compared with maintaining their full matrices, resulting in reduced peak memory usage. Secondly, the preconditioner L_k recovered from $L_k = \mathcal{D}(\bar{C}_k^L) \mathcal{D}(\bar{C}_k^L)^T$ is naturally symmetric and positive definite, and thus satisfies the intrinsic theoretical properties of its high-precision 32-bit version, thereby reducing information loss. Fig. 2 shows that Cholesky quantization significantly improves the test accuracy of the vanilla 4-bit Shampoo, and saves peak memory cost at the same time.

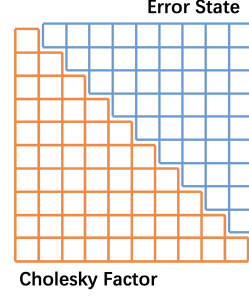


Figure 3. Efficient storage for Cholesky factor and error state.

4.3. Compensated Cholesky Quantization

To mitigate the information loss from quantization, we introduce error feedback (EF) for Cholesky factors. Error feedback was originally proposed to alleviate the information loss caused by gradient compression for communication in distributed training setting [38, 40]. The key idea is to compensate for compression errors by adding them back into the gradients before compression in the next step. Practical adaptations of EF has also been explored in [44, 53] to combine EF with adaptive gradient methods for communication-efficient large-scale training.

Different from previous work, our focus in this work is the compression of preconditioners of preconditioned gradient methods, and therefore our error feedback is conducted on the preconditioners. At each iteration, an additional low-precision (4-bit) error state, denoted as \bar{E}_k^L , is maintained to capture quantization error for the Cholesky factor \bar{C}_k^L . This error state is then used in the next iteration to enhance precision by compensating for potential quantization errors.

Specifically, at iteration k , we first compute the Cholesky factors C_k^L and C_k^R following the standard steps in Eq. (5). Before quantizing, we apply error compensation as follows:

$$\begin{aligned}
 E_{k-1}^L &= \mathcal{D}(\bar{E}_{k-1}^L), & \bar{C}_k^L &= \mathcal{Q}(C_k^L + E_{k-1}^L), \\
 E_{k-1}^R &= \mathcal{D}(\bar{E}_{k-1}^R), & \bar{C}_k^R &= \mathcal{Q}(C_k^R + E_{k-1}^R).
 \end{aligned} \tag{7}$$

Next, we update the error states \bar{E}_k^L and \bar{E}_k^R using an exponential moving average to improve stability:

$$\begin{aligned}
 E_k^L &= \beta_e E_{k-1}^L + (1 - \beta_e)(C_k^L + E_{k-1}^L - \mathcal{D}(\bar{C}_k^L)), \\
 E_k^R &= \beta_e E_{k-1}^R + (1 - \beta_e)(C_k^R + E_{k-1}^R - \mathcal{D}(\bar{C}_k^R)),
 \end{aligned} \tag{8}$$

where β_e is a momentum parameter. Since the Cholesky factors C_k^L and C_k^R are lower triangular matrices, and quantization excludes diagonal elements, the error matrices E_k^L and E_k^R are also triangular with zero diagonal entries. This structure allows for efficient storage, as we can store each error matrix as the upper triangular part as illustrated in Fig. 3, imposing no additional memory overhead compared with vanilla 4-bit Shampoo.

Finally, we can compute the inverse 1/4-th root of the

Algorithm 1 4-bit Shampoo via Compensated Cholesky Quantization

Input: initial weight $W_0 \in \mathbb{R}^{m \times n}$, initial Cholesky factors $\bar{C}_0^L = \sqrt{\epsilon}I_m$, $\bar{C}_0^R = \sqrt{\epsilon}I_n$, quantization error states $\bar{E}_0^L = \mathbf{0}$, $\bar{E}_0^R = \mathbf{0}$, initial preconditioners $\hat{L}_0 = I_m$, $\hat{R}_0 = I_n$. Total training iterations T , interval of updating preconditioners T_1 and T_2 , momentum parameter $\beta, \beta_e \in (0, 1)$. First-order optimizer \mathcal{F} with initial optimizer state s_0 .

Output: final weight W_T .

```

1: for  $k = 1, 2, \dots, T$  do
2:   Compute gradient  $G_k = \nabla \mathcal{L}_k(W_k)$ 
3:   if  $k \% T_1 \equiv 0$  then
4:     Update Cholesky factors according to Eq. (5)
5:     Conduct error compensation following Eq. (7)
6:     Update quantization error states as Eq. (8)
7:   else
8:      $\bar{C}_k^L = \bar{C}_{k-1}^L$ ,  $\bar{C}_k^R = \bar{C}_{k-1}^R$ 
9:   end if
10:  if  $k \% T_2 \equiv 0$  then
11:    Compute inverse 1/4-th root of the preconditioners following Eq. (9)
12:  else
13:     $\hat{L}_k = \hat{L}_{k-1}$ ,  $\hat{R}_k = \hat{R}_{k-1}$ 
14:  end if
15:   $\hat{G}_k = \mathcal{D}(\hat{L}_k)G_k\mathcal{D}(\hat{R}_k)$ 
16:   $W_k, s_k = \mathcal{F}(W_{k-1}, s_{k-1}, \hat{G}_k)$ 
17: end for

```

preconditioners with stored Cholesky factors via

$$\begin{aligned} \hat{L}_k &= \mathcal{Q}((\mathcal{D}(\bar{C}_k^L)\mathcal{D}(\bar{C}_k^L)^T + \lambda_{\max}^L \epsilon I_m)^{-1/4}), \\ \hat{R}_k &= \mathcal{Q}((\mathcal{D}(\bar{C}_k^R)\mathcal{D}(\bar{C}_k^R)^T + \lambda_{\max}^R \epsilon I_n)^{-1/4}). \end{aligned} \quad (9)$$

Next, with SGD as the base optimizer, the model parameters are updated with the preconditioned gradient:

$$W_{k+1} = W_k - \eta_k \mathcal{D}(\hat{L}_k)G_k\mathcal{D}(\hat{R}_k), \quad (10)$$

where η_k is the learning rate for iteration k that is often scaled by $\|G_k\|_F / \|\hat{G}_k\|_F$ according to the grafting trick [1]. The preconditioned stochastic gradient $\mathcal{D}(\hat{L}_k)G_k\mathcal{D}(\hat{R}_k)$ can also be fed into another first-order optimizer \mathcal{F} , such as Adam, for model updates. Accordingly, we have arrived at our compensated Cholesky quantization based Shampoo summarized in Algorithm 1.

5. Theoretical Analysis

Here we provide theoretical analysis of Algorithm 1 with SGD base optimizer as an example. We first define

$$\begin{aligned} x_k &:= \text{Vec}(W_k), \quad g_k := \text{Vec}(G_k), \\ H_k &:= \mathcal{D}(\hat{R}_k) \otimes \mathcal{D}(\hat{L}_k), \end{aligned} \quad (11)$$

where Vec reshapes the matrix into a vector by concatenating the columns of the matrix. Then, we rewrite Shampoo with SGD as base optimizer in Eq. (10) into an equivalent

vectorization formulation:

$$x_{k+1} = x_k - \eta_k H_k g_k. \quad (12)$$

See this equivalent derivation in Appendix B. In the following, we analyze Shampoo with SGD as base optimizer in Eq. (12) under different situations.

5.1. Smooth Nonconvex Training Loss

Here we analyze the smooth nonconvex f , which is defined according to loss function Eq. (1) as

$$f(x) := F(W), \quad (13)$$

where $x = \text{Vec}(W)$ is the vectorized model parameter. To this end, we introduce the necessary assumptions.

Assumption 5.1. *a) Assume the training loss f is L -Lipschitz smooth, i.e., $\|\nabla f(x) - \nabla f(y)\|_2 \leq L\|x - y\|_2$. b) Suppose the stochastic gradient g_k is unbiased and its variance can be bounded: $\mathbb{E}[g_k] = \nabla f(x_k)$ and $\mathbb{E}[\|g_k - \nabla f(x_k)\|_2^2] \leq \sigma^2(1 + \|\nabla f(x_k)\|_2^2)$. c) Assume the preconditioner H_k has bounded eigenvalues, i.e., $\sup_k \lambda_{\max}(H_k) \leq \lambda_{H, \max} < \infty$ and $\inf_k \lambda_{\min}(H_k) \geq \lambda_{H, \min} > 0$.*

For Assumptions 5.1a) and b), they are standard for stochastic first-order methods. Indeed, Assumption 5.1b) is even weaker than the commonly assumed bounded variance condition $\mathbb{E}[\|g_k - \nabla f(x_k)\|_2^2] \leq \sigma^2$. Assumption 5.1c) requires that the preconditioner H_k be positive definite and bounded, which can be partially explained by the following Proposition 5.1.

Proposition 5.1. *For the 4-bit Shampoo in Algorithm 1, if $\|(\mathcal{D}(\bar{C}_k^L)\mathcal{D}(\bar{C}_k^L)^T + \lambda_{\max}^L \epsilon I_m)^{-1/4}\|_{\text{off}, \max} \leq C_B$, then its preconditioners hold that*

$$\begin{aligned} \mathcal{D}(\hat{L}_k) &\succeq (\mathcal{D}(\bar{C}_k^L)\mathcal{D}(\bar{C}_k^L)^T + \lambda_{\max}^L \epsilon I_m)^{-1/4} - C_B n_k 2^{-b} I, \\ \mathcal{D}(\hat{L}_k) &\preceq (\mathcal{D}(\bar{C}_k^L)\mathcal{D}(\bar{C}_k^L)^T + \lambda_{\max}^L \epsilon I_m)^{-1/4} + C_B n_k 2^{-b} I, \end{aligned}$$

where $\lambda_{\max}^L = \lambda_{\max}(\mathcal{D}(\bar{C}_k^L)\mathcal{D}(\bar{C}_k^L)^T)$ and $\lambda_{\max}^R = \lambda_{\max}(\mathcal{D}(\bar{C}_k^R)\mathcal{D}(\bar{C}_k^R)^T)$, and $\|\cdot\|_{\text{off}, \max}$ denotes the maximal absolute value of off-diagonal entries in each quantization partition blocks. $b = 4$ is the quantization bit-width, and n_k is the number of rows in W_k .

This proposition shows that the sequence $\{\mathcal{D}(\hat{L}_k)\}$ can be bounded above and below. Below, we analyze the distribution of the eigenvalues of the dequantized preconditioners $\mathcal{D}(\hat{L}_k)$ and $\mathcal{D}(\hat{R}_k)$ during the training process to further validate Assumption 5.1c). We can see from Fig. 4 that all the eigenvalues of the dequantized preconditioners $\mathcal{D}(\hat{L})$ and $\mathcal{D}(\hat{R})$ are positive during the training process.

Now we are ready to derive the convergence, and state the main results below.

Theorem 5.1. *Suppose Assumption 5.1 holds. Let $\eta_k = \frac{c}{\sqrt{T+1}}$ with $c \in \left(0, \frac{\lambda_{H, \min}}{2L(1+\sigma^2)\lambda_{H, \max}^2}\right)$, then we have*

$$\mathbb{E} \left[\|\nabla f(\bar{x}_T)\|_2^2 \right] \leq \frac{2(f(x_0) - \bar{f} + c^2 L \sigma^2 \lambda_{H, \max}^2)}{c \lambda_{H, \min} \sqrt{T+1}},$$

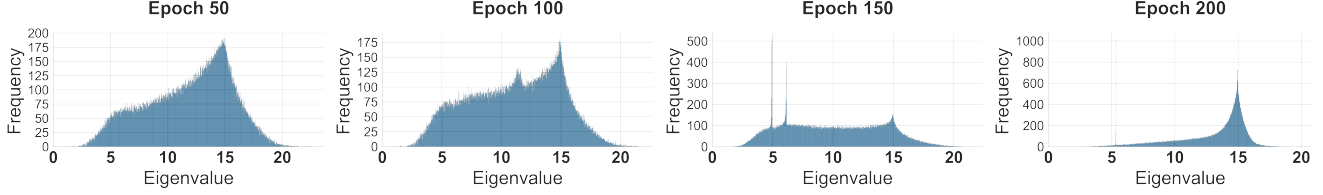


Figure 4. Eigenvalue frequency of the dequantized preconditioners $\mathcal{D}(\hat{L})$ and $\mathcal{D}(\hat{R})$ of VGG-19 on CIFAR-100 at 50, 100, 150, and 200 training epochs, all eigenvalues are greater than 0.

where \bar{x}_T is randomly selected from $\{x_0, x_1, \dots, x_T\}$ and $\bar{f} := \min_{x \in \mathbb{R}^d} f(x)$.

See its proof in Appendix B. Theorem 5.1 shows that for smooth nonconvex training loss, our 4-bit Shampoo with SGD as the base optimizer can converge at the rate of $\mathcal{O}(\frac{1}{\sqrt{T}})$. This convergence rate is optimal as shown in [8], indicating the high efficiency of our proposed Algorithm 1.

5.2. Nonsmooth Nonconvex Training Loss

In this subsection, we analyze the nonsmooth nonconvex training loss function, particularly in cases where the activation function is nonsmooth, such as the ReLU in ResNet [23]. The iterative scheme can be written as:

$$x_{k+1} = x_k - \eta_k H_k(d_k + \xi_k),$$

where $d_k \in \partial f(x_k)$, ∂f denotes the subgradient of f , and $\{\xi_k\}$ is the sequence of the random noise in the subgradient. Relevant concepts are provided in Appendix B.2. Given a process $\{\xi_i\}_{i=0}^{\infty}$, let \mathcal{F}_k denote the history up to iteration k . To this end, we introduce the necessary assumptions.

Assumption 5.2. a) The function f is ℓ -Lipschitz continuous. Additionally, f is a Whitney stratifiable function.

b) The noise in the subgradient is unbiased and has bounded variance

$$\mathbb{E}[\xi_k | \mathcal{F}_{k-1}] = 0, \quad \mathbb{E}[\|\xi_k\|_2^2 | \mathcal{F}_{k-1}] \leq \sigma^2,$$

c) For any convergent subsequence $x_{k_j} \rightarrow \bar{x}$, we have $\lim_{N \rightarrow \infty} \frac{1}{N} \sum_{j=1}^N H_{k_j} = \bar{H}$ for some positive definite matrix \bar{H} . Additionally, $\sup_{k \geq 0} \lambda_{\max}(H_k) \leq M$.

The class of Lipschitz continuous functions is broad and includes pathological cases where subgradient flows fail to converge to stationary points [12]. To address this, we focus on Whitney stratifiable functions, which generalize most practical cases, including loss functions in neural networks with nonsmooth activations like ReLU [5, 13]. Assumption 5.2c) requires only Cesàro summability of $\{H_k\}$, a mild condition crucial for handling non-time-homogeneity.

Theorem 5.2. Suppose that Assumption 5.2 holds and the sequence $\{x_k\}$ remains within a compact set. If the learning rate satisfies $\sum_{k=1}^{\infty} \eta_k = \infty$ and $\sum_{k=1}^{\infty} \eta_k^2 < \infty$, then

$$\lim_{k \rightarrow \infty} \text{dist}(x_k, \Omega) = 0,$$

where $\Omega := \{x : 0 \in \partial f(x)\}$ is the set of stationary points.

For a stratifiable function, the result of convergence to the stationary point set is tight. There are no complexity

results due to the challenges posed by its complex nonconvexity and nonsmoothness [5, 13]. This result ensures the convergence of our proposed algorithm on nonsmooth training losses, including those arising in deep neural networks such as ReLU-based architectures.

6. Experiments

In this section, we conduct experiments to compare the performance of our 4-bit Shampoo Algorithm 1 with vanilla 4-bit and 32-bit Shampoo when using SGD with momentum (SGDM) [43] or AdamW [34] as the base optimizer, and the base optimizer themselves. For all the experiments, we record test accuracy, wall-clock time, and peak memory usage to comprehensively assess algorithm performance, computational overhead, and GPU memory overhead.

Training Setting Following standard benchmarks for image classification [23, 31, 50], we train VGG-19 [42], ResNet-34 [23], Swin Transformer Tiny (Swin-Tiny) [33], and Vision Transformer Small (ViT-Small) [16] on CIFAR-100 [27] and Tiny-ImageNet [29], and ResNet-50 on ImageNet [14]. For data augmentation, we apply horizontal flip, random crop, and color jitter for VGG and ResNet [23, 28], and Mixup [58], CutMix [57], RandomErasing [60], and RandAugment/AutoAugment [10, 11] for Swin and ViT [31, 33]. Training hyperparameters for Shampoo match the base optimizer, except the base optimizer is trained for additional epochs to achieve comparable performance. All experiments were conducted on a single A100 GPU. Further experimental details are provided in Appendix C.

Test Performance To make a fair comparison of vanilla 4-bit Shampoo and our algorithms, we apply off-diagonal 4-bit block-wise quantization to Shampoo’s preconditioners for storage and take this as the vanilla 4-bit Shampoo. As shown in Tab. 4, off-diagonal quantization only slightly increases peak memory usage but improves the test performance. Consequently, we use off-diagonal block-wise quantization for vanilla 4-bit Shampoo in all experiments.

As shown in Tab. 1, 4-bit Shampoo with Cholesky quantization consistently outperforms vanilla 4-bit Shampoo. For instance, with SGDM as the base optimizer for training ResNet-34 on CIFAR-100, it achieves 80.27% test accuracy compared to 79.45% for vanilla 4-bit Shampoo. Similarly, with AdamW as the base optimizer for ViT-Small on CIFAR-100, it reaches 76.50% test accuracy versus 74.56%

Table 1. Test accuracy (%), wall-clock time (min), and peak memory (MB) comparison on CIFAR-100 dataset. Here VQ denotes vanilla quantization, CQ denotes Cholesky quantization, and EF denotes error feedback.

Model	Optimizer	Accuracy	Time	Memory
VGG-19	SGDM	74.43	35.8	597.3
	SGDM+32-bit Shampoo	75.02	31.4	1065.2
	SGDM+4-bit Shampoo (VQ)	74.36	31.9	662.2
	SGDM+4-bit Shampoo (CQ)	74.99	32.9	646.0
	SGDM+4-bit Shampoo (CQ+EF)	75.21	33.2	662.2
ResNet-34	SGDM	79.12	60.9	1254.7
	SGDM+32-bit Shampoo	80.69	53.1	1882.6
	SGDM+4-bit Shampoo (VQ)	79.45	54.0	1341.0
	SGDM+4-bit Shampoo (CQ)	80.27	55.8	1319.5
	SGDM+4-bit Shampoo (CQ+EF)	80.52	56.1	1341.0
Swin-Tiny	AdamW	78.28	163.0	1095.3
	AdamW+32-bit Shampoo	79.84	138.4	1248.6
	AdamW+4-bit Shampoo (VQ)	78.33	140.1	1116.8
	AdamW+4-bit Shampoo (CQ)	79.29	143.4	1111.5
	AdamW+4-bit Shampoo (CQ+EF)	79.45	146.7	1116.8
ViT-Small	AdamW	73.00	311.2	2930.0
	AdamW+32-bit Shampoo	78.21	230.3	3448.9
	AdamW+4-bit Shampoo (VQ)	74.56	235.9	3001.7
	AdamW+4-bit Shampoo (CQ)	76.50	239.3	2983.7
	AdamW+4-bit Shampoo (CQ+EF)	76.76	239.8	3001.7

Table 2. Test accuracy (%), wall-clock time (min), and peak memory (MB) comparison on Tiny-ImageNet dataset. Here VQ denotes vanilla quantization, CQ denotes Cholesky quantization, and EF denotes error feedback.

Model	Optimizer	Accuracy	Time	Memory
VGG-19	SGDM	62.19	86.3	1632.8
	SGDM+32-bit Shampoo	63.36	66.7	2102.5
	SGDM+4-bit Shampoo (VQ)	62.34	67.1	1697.8
	SGDM+4-bit Shampoo (CQ+EF)	63.51	69.6	1697.8
ResNet-34	SGDM	68.27	189.7	4221.3
	SGDM+32-bit Shampoo	69.11	139.1	4846.0
	SGDM+4-bit Shampoo (VQ)	68.43	139.6	4307.7
	SGDM+4-bit Shampoo (CQ+EF)	68.88	141.1	4307.7
Swin-Tiny	AdamW	60.74	317.1	1105.5
	AdamW+32-bit Shampoo	62.73	255.3	1256.8
	AdamW+4-bit Shampoo (VQ)	61.28	277.6	1126.9
	AdamW+4-bit Shampoo (CQ+EF)	61.91	283.4	1126.9
ViT-Small	AdamW	55.21	601.7	2944.2
	AdamW+32-bit Shampoo	58.11	449.6	3468.1
	AdamW+4-bit Shampoo (VQ)	56.47	456.6	3016.0
	AdamW+4-bit Shampoo (CQ+EF)	57.45	462.4	3016.0

for vanilla 4-bit Shampoo. This performance improvement arises from Cholesky quantization’s ability to recover pre-conditioners from Cholesky factors, thereby preserving the symmetry and positive definiteness of the original 32-bit Shampoo preconditioners, as detailed in Sec. 4.2.

Moreover, experimental results in Tab. 1 validate the effectiveness of the error compensation strategy for Cholesky factors introduced in Sec. 4.3. Specifically, with SGDM as the base optimizer for ResNet-34 on CIFAR-100, 4-bit Shampoo with compensated Cholesky decomposition improves test accuracy by 0.25% compared to 4-bit Cholesky quantization. Similarly, with AdamW as the base optimizer for ViT-Small on CIFAR-100, it achieves a 0.26% test accuracy improvement. This consistent gain is due to the er-

ror feedback compensation applied to the 4-bit Cholesky factors. By retaining and integrating quantization errors from previous steps into the updated Cholesky factors before each quantization, the strategy effectively minimizes quantization errors iteratively.

Experimental results on larger datasets, as shown in Tabs. 2 and 3, further validates the superiority of our proposed 4-bit Shampoo with compensated Cholesky quantization. On Tiny-ImageNet, it consistently improves test accuracy by over 0.45% compared to vanilla 4-bit Shampoo, whether using SGDM or AdamW as the base optimizer. For ResNet-50 on ImageNet with SGDM, it boosts test accuracy by 0.27% over vanilla 4-bit Shampoo, achieving performance within 0.06% of the original 32-bit Shampoo.

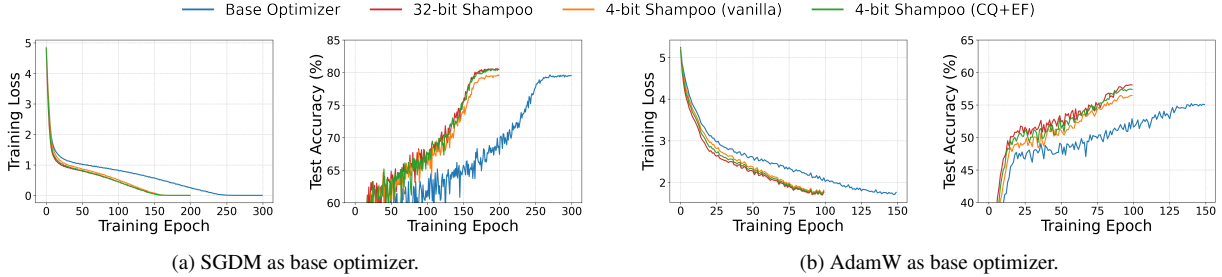


Figure 5. Comparison of training loss and test accuracy (%) for training ResNet-34 on CIFAR-100 and ViT-Small on Tiny-ImageNet. The left figure shows ResNet-34 results, and the right figure shows ViT-Small results.

Table 3. Test accuracy (%), wall-clock time (min), and peak memory (MB) comparison on ImageNet dataset. Here VQ denotes vanilla quantization, CQ denotes Cholesky quantization, and EF denotes error feedback.

Model	Optimizer	Accuracy	Time	Memory
ResNet-50	SGDM	77.56	2106.4	11356.2
	SGDM+32-bit Shampoo	78.06	1841.1	11986.4
	SGDM+4-bit Shampoo (VQ)	77.73	1882.8	11445.2
	SGDM+4-bit Shampoo (CQ+EF)	78.00	1899.4	11455.2

Table 4. Comparison of test accuracy (%) and peak memory usage (MB) for vanilla 4-bit Shampoo with off-diagonal and original block-wise quantization with VGG-19 on CIFAR-100 and Swin-Tiny on Tiny-ImageNet.

Model	VGG-19		Swin-Tiny	
	Accuracy	Memory	Accuracy	Memory
Original	74.20	661.7	60.83	1126.2
Off-Diagonal	74.36	662.2	61.28	1126.9

Memory and Computing Efficiency For GPU memory usage, Tabs. 1 to 3 show that 4-bit quantization substantially reduces the peak memory usage of the original 32-bit Shampoo. For instance, with SGDM as the base optimizer for training ResNet-34 on CIFAR-100, 4-bit Shampoo decreases peak memory usage by more than 540MB compared to its 32-bit counterpart. Similarly, with AdamW as the base optimizer for ViT-Small on Tiny-ImageNet, 4-bit Shampoo saves over 450MB peak memory usage.

Moreover, Tab. 1 shows that 4-bit Cholesky quantization achieves lower peak GPU memory usage than vanilla 4-bit Shampoo. For instance, when training ResNet-34 on CIFAR-100 with SGDM as the base optimizer, 4-bit Shampoo with Cholesky quantization reduces peak memory usage by an additional 21.5MB compared to vanilla 4-bit Shampoo. Similarly, with AdamW as the base optimizer for ViT-Small on CIFAR-100, Cholesky quantization provides a further 18.0MB reduction. The reduced peak GPU memory of Cholesky quantization accounts for approximately 25% of the total extra GPU memory overhead introduced by the preconditioners of vanilla 4-bit Shampoo. As detailed in Sec. 4.2, this memory efficiency stems from Cholesky quantization operating on the lower triangular Cholesky factors, where storing $\tilde{C}_k^L, \tilde{C}_k^R$ requires roughly half the memory of storing full matrices L_k, R_k . Consequently, 4-bit Sham-

poo with Cholesky quantization achieves additional memory savings over the vanilla 4-bit quantization approach. See more discussions in Appendix C.

For computing efficiency, Tabs. 1 to 3 show that the additional computing time brought by compensated Cholesky quantization compared with the vanilla 4-bit quantization is small. Even when training ResNet-50 on ImageNet, the additional computing time is only less than 17 minutes, whereas the total training time more than 31 hours.

Moreover, despite longer training times and more epochs with base optimizers SGDM and AdamW, their test accuracy remains below Shampoo as shown in Fig. 5. Detailed experimental settings can be found in Appendix C.

7. Conclusion

We introduce 4-bit Shampoo, a memory-efficient, 4-bit preconditioned gradient method that greatly reduces GPU memory usage while retaining performance comparable to 32-bit Shampoo. By applying Cholesky quantization, we store only 4-bit lower triangular Cholesky factors, which cuts memory costs in half and preserves the symmetry and positive definiteness of preconditioners. An error feedback mechanism further reduces quantization loss by compensating for quantization error at each step. Our approach, which we prove to converge in nonconvex settings, demonstrates strong performance on image classification benchmarks.

Limitations. (a) Our proposed Cholesky quantization and error feedback strategy were only tested with Shampoo, though they are general for preconditioning matrices and could be applied to other preconditioned gradient methods, which we leave for future work. (b) Due to limited GPU resources, we evaluated our 4-bit Shampoo with compensated Cholesky quantization only on ResNet-50 for ImageNet. Future work will test it on ViTs for ImageNet.

References

- [1] Naman Agarwal, Rohan Anil, Elad Hazan, Tomer Koren, and Cyril Zhang. Disentangling adaptive gradient methods from learning rates. *arXiv preprint arXiv:2002.11803*, 2020. 5
- [2] Dan Alistarh, Demjan Grubic, Jerry Li, Ryota Tomioka, and Milan Vojnovic. Qsgd: Communication-efficient sgd via gradient quantization and encoding. *Advances in neural information processing systems*, 30, 2017. 2
- [3] Rohan Anil, Vineet Gupta, Tomer Koren, Kevin Regan, and Yoram Singer. Scalable second order optimization for deep learning. *arXiv preprint arXiv:2002.09018*, 2020. 1, 2
- [4] Michel Benaïm, Josef Hofbauer, and Sylvain Sorin. Stochastic approximations and differential inclusions. *SIAM J. Control and Optimization*, 44(1):328–348, 2005. 2, 3
- [5] Jérôme Bolte and Edouard Pauwels. Conservative set valued fields, automatic differentiation, stochastic gradient methods and deep learning. *Mathematical Programming*, 188:19–51, 2021. 6
- [6] Vivek S Borkar. *Stochastic approximation: a dynamical systems viewpoint*. Springer, 2009. 3
- [7] Tom B Brown. Language models are few-shot learners. *arXiv preprint arXiv:2005.14165*, 2020. 1
- [8] Yair Carmon, John C Duchi, Oliver Hinder, and Aaron Sidford. Lower bounds for finding stationary points ii: first-order methods. *Mathematical Programming*, 185(1):315–355, 2021. 6
- [9] Frank H Clarke. *Optimization and nonsmooth analysis*. SIAM, 1990. 2
- [10] Ekin D Cubuk, Barret Zoph, Dandelion Mane, Vijay Vasudevan, and Quoc V Le. Autoaugment: Learning augmentation policies from data. *arXiv preprint arXiv:1805.09501*, 2018. 6
- [11] Ekin D Cubuk, Barret Zoph, Jonathon Shlens, and Quoc V Le. Randaugment: Practical automated data augmentation with a reduced search space. In *Proceedings of the IEEE/CVF conference on computer vision and pattern recognition workshops*, pages 702–703, 2020. 6
- [12] Aris Daniilidis and Dmitriy Drusvyatskiy. Pathological subgradient dynamics. *SIAM Journal on Optimization*, 30(2):1327–1338, 2020. 6
- [13] Damek Davis, Dmitriy Drusvyatskiy, Sham Kakade, and Jason D Lee. Stochastic subgradient method converges on tame functions. *Foundations of Computational Mathematics*, 20(1):119–154, 2020. 6, 2, 3
- [14] Jia Deng, Wei Dong, Richard Socher, Li-Jia Li, Kai Li, and Li Fei-Fei. Imagenet: A large-scale hierarchical image database. In *2009 IEEE conference on computer vision and pattern recognition*, pages 248–255. Ieee, 2009. 6
- [15] Tim Dettmers, Mike Lewis, Sam Shleifer, and Luke Zettlemoyer. 8-bit optimizers via block-wise quantization. *arXiv preprint arXiv:2110.02861*, 2021. 2, 3
- [16] Alexey Dosovitskiy, Lucas Beyer, Alexander Kolesnikov, Dirk Weissenborn, Xiaohua Zhai, Thomas Unterthiner, Mostafa Dehghani, Matthias Minderer, Georg Heigold, Sylvain Gelly, et al. An image is worth 16x16 words: Transformers for image recognition at scale. In *International Conference on Learning Representations*, 2020. 1, 3, 6
- [17] John Duchi, Elad Hazan, and Yoram Singer. Adaptive subgradient methods for online learning and stochastic optimization. *Journal of Machine Learning Research*, 12(7), 2011. 1, 2
- [18] John C Duchi and Feng Ruan. Stochastic methods for composite and weakly convex optimization problems. *SIAM J. Optimization*, 28(4):3229–3259, 2018. 3
- [19] Amir Gholami, Sehoon Kim, Zhen Dong, Zhewei Yao, Michael W Mahoney, and Kurt Keutzer. A survey of quantization methods for efficient neural network inference. In *Low-Power Computer Vision*, pages 291–326. Chapman and Hall/CRC, 2022. 3
- [20] Donald Goldfarb, Yi Ren, and Achraf Bahamou. Practical quasi-newton methods for training deep neural networks. *Advances in Neural Information Processing Systems*, 33:2386–2396, 2020. 1, 2
- [21] Chun-Hua Guo and Nicholas J Higham. A schur–newton method for the matrix p th root and its inverse. *SIAM Journal on Matrix Analysis and Applications*, 28(3):788–804, 2006. 3
- [22] Vineet Gupta, Tomer Koren, and Yoram Singer. Shampoo: Preconditioned stochastic tensor optimization. In *International Conference on Machine Learning*, pages 1842–1850. PMLR, 2018. 1, 2
- [23] Kaiming He, Xiangyu Zhang, Shaoqing Ren, and Jian Sun. Deep residual learning for image recognition. In *Proceedings of the IEEE Conference on Computer Vision and Pattern Recognition*, pages 770–778, 2016. 1, 2, 6, 4
- [24] Jordan Hoffmann, Sebastian Borgeaud, Arthur Mensch, Elena Buchatskaya, Trevor Cai, Eliza Rutherford, Diego de Las Casas, Lisa Anne Hendricks, Johannes Welbl, Aidan Clark, et al. Training compute-optimal large language models. *arXiv preprint arXiv:2203.15556*, 2022. 1
- [25] Jared Kaplan, Sam McCandlish, Tom Henighan, Tom B Brown, Benjamin Chess, Rewon Child, Scott Gray, Alec Radford, Jeffrey Wu, and Dario Amodei. Scaling laws for neural language models. *arXiv preprint arXiv:2001.08361*, 2020. 1
- [26] Diederik P Kingma. Adam: A method for stochastic optimization. *arXiv preprint arXiv:1412.6980*, 2014. 1, 2
- [27] Alex Krizhevsky, Geoffrey Hinton, et al. Learning multiple layers of features from tiny images. 2009. 3, 6
- [28] Alex Krizhevsky, Ilya Sutskever, and Geoffrey E Hinton. Imagenet classification with deep convolutional neural networks. *Advances in neural information processing systems*, 25, 2012. 6
- [29] Ya Le and Xuan Yang. Tiny imagenet visual recognition challenge. *CS 231N*, 7(7):3, 2015. 6
- [30] Jinhyuk Lee, Wonjin Yoon, Sungdong Kim, Donghyeon Kim, Sunkyu Kim, Chan Ho So, and Jaewoo Kang. Biobert: a pre-trained biomedical language representation model for biomedical text mining. *Bioinformatics*, 36(4):1234–1240, 2020. 1
- [31] Seung Hoon Lee, Seunghyun Lee, and Byung Cheol Song. Vision transformer for small-size datasets. *arXiv preprint arXiv:2112.13492*, 2021. 6, 4

- [32] Bingrui Li, Jianfei Chen, and Jun Zhu. Memory efficient optimizers with 4-bit states. *Advances in Neural Information Processing Systems*, 36, 2024. 2, 3
- [33] Ze Liu, Yutong Lin, Yue Cao, Han Hu, Yixuan Wei, Zheng Zhang, Stephen Lin, and Baining Guo. Swin transformer: Hierarchical vision transformer using shifted windows. In *Proceedings of the IEEE/CVF International Conference on Computer Vision*, pages 10012–10022, 2021. 1, 6, 4
- [34] Ilya Loshchilov and Frank Hutter. Decoupled weight decay regularization. In *International Conference on Learning Representations*, 2019. 1, 6
- [35] James Martens and Roger Grosse. Optimizing neural networks with kronecker-factored approximate curvature. In *International Conference on Machine Learning*, pages 2408–2417. PMLR, 2015. 1, 2
- [36] Depen Morwani, Itai Shapira, Nikhil Vyas, Eran Malach, Sham Kakade, and Lucas Janson. A new perspective on shampoo’s preconditioner. *arXiv preprint arXiv:2406.17748*, 2024. 2
- [37] Alec Radford, Jong Wook Kim, Chris Hallacy, Aditya Ramesh, Gabriel Goh, Sandhini Agarwal, Girish Sastry, Amanda Askell, Pamela Mishkin, Jack Clark, et al. Learning transferable visual models from natural language supervision. In *International conference on machine learning*, pages 8748–8763. PMLR, 2021. 1
- [38] Peter Richtárik, Igor Sokolov, and Ilyas Fatkhullin. Ef21: A new, simpler, theoretically better, and practically faster error feedback. *Advances in Neural Information Processing Systems*, 34:4384–4396, 2021. 2, 4
- [39] Herbert Robbins and Sutton Monro. A stochastic approximation method. *The Annals of Mathematical Statistics*, pages 400–407, 1951. 1
- [40] Frank Seide, Hao Fu, Jasha Droppo, Gang Li, and Dong Yu. 1-bit stochastic gradient descent and its application to data-parallel distributed training of speech dnns. In *Interspeech*, pages 1058–1062. Singapore, 2014. 2, 4
- [41] Hao-Jun Michael Shi, Tsung-Hsien Lee, Shintaro Iwasaki, Jose Gallego-Posada, Zhijing Li, Kaushik Rangadurai, Dheevatsa Mudigere, and Michael Rabbat. A distributed data-parallel pytorch implementation of the distributed shampoo optimizer for training neural networks at-scale. *arXiv preprint arXiv:2309.06497*, 2023. 1, 2
- [42] Karen Simonyan and Andrew Zisserman. Very deep convolutional networks for large-scale image recognition. *arXiv preprint arXiv:1409.1556*, 2014. 6
- [43] Ilya Sutskever, James Martens, George Dahl, and Geoffrey Hinton. On the importance of initialization and momentum in deep learning. In *International Conference on Machine Learning*, pages 1139–1147. PMLR, 2013. 1, 6
- [44] Hanlin Tang, Shaoduo Gan, Ammar Ahmad Awan, Samyam Rajbhandari, Conglong Li, Xiangru Lian, Ji Liu, Ce Zhang, and Yuxiong He. 1-bit adam: Communication efficient large-scale training with adam’s convergence speed. In *International Conference on Machine Learning*, pages 10118–10129. PMLR, 2021. 2, 4
- [45] Tijmen Tieleman, Geoffrey Hinton, et al. Lecture 6.5-rmsprop: Divide the gradient by a running average of its recent magnitude. *COURSERA: Neural networks for machine learning*, 4(2):26–31, 2012. 2
- [46] Hugo Touvron, Thibaut Lavril, Gautier Izacard, Xavier Martinet, Marie-Anne Lachaux, Timothée Lacroix, Baptiste Rozière, Naman Goyal, Eric Hambro, Faisal Azhar, et al. Llama: Open and efficient foundation language models. *arXiv preprint arXiv:2302.13971*, 2023. 1
- [47] Thijs Vogels, Sai Praneeth Karimireddy, and Martin Jaggi. Powersgd: Practical low-rank gradient compression for distributed optimization. *Advances in Neural Information Processing Systems*, 32, 2019. 2
- [48] Nikhil Vyas, Depen Morwani, Rosie Zhao, Itai Shapira, David Brandfonbrener, Lucas Janson, and Sham Kakade. Soap: Improving and stabilizing shampoo using adam. *arXiv preprint arXiv:2409.11321*, 2024. 2
- [49] Wei Wen, Cong Xu, Feng Yan, Chunpeng Wu, Yandan Wang, Yiran Chen, and Hai Li. Terngrad: Ternary gradients to reduce communication in distributed deep learning. *Advances in neural information processing systems*, 30, 2017. 2
- [50] Ross Wightman, Hugo Touvron, and Hervé Jégou. Resnet strikes back: An improved training procedure in timm. *arXiv preprint arXiv:2110.00476*, 2021. 6
- [51] Shijie Wu, Ozan Irsoy, Steven Lu, Vadim Dabravolski, Mark Dredze, Sebastian Gehrmann, Prabhanjan Kambadur, David Rosenberg, and Gideon Mann. Bloomberggpt: A large language model for finance. *arXiv preprint arXiv:2303.17564*, 2023. 1
- [52] Tian Xie and Jeffrey C Grossman. Crystal graph convolutional neural networks for an accurate and interpretable prediction of material properties. *Physical review letters*, 120(14):145301, 2018. 1
- [53] Xingyu Xie, Zhijie Lin, Kim-Chuan Toh, and Pan Zhou. Loco: Low-bit communication adaptor for large-scale model training. *arXiv preprint arXiv:2407.04480*, 2024. 2, 4
- [54] Xingyu Xie, Pan Zhou, Huan Li, Zhouchen Lin, and Shuicheng Yan. Adan: Adaptive nesterov momentum algorithm for faster optimizing deep models. *IEEE Transactions on Pattern Analysis and Machine Intelligence*, 2024. 1, 4
- [55] Zhewei Yao, Reza Yazdani Aminabadi, Minjia Zhang, Xiaoxia Wu, Conglong Li, and Yuxiong He. Zeroquant: Efficient and affordable post-training quantization for large-scale transformers. *Advances in Neural Information Processing Systems*, 35:27168–27183, 2022. 3
- [56] Hongwei Yong, Ying Sun, and Lei Zhang. A general regret bound of preconditioned gradient method for dnn training. In *Proceedings of the IEEE/CVF Conference on Computer Vision and Pattern Recognition*, pages 7866–7875, 2023. 1, 2, 3
- [57] Sangdoon Yun, Dongyoon Han, Seong Joon Oh, Sanghyuk Chun, Junsuk Choe, and Youngjoon Yoo. Cutmix: Regularization strategy to train strong classifiers with localizable features. In *Proceedings of the IEEE/CVF international conference on computer vision*, pages 6023–6032, 2019. 6
- [58] Hongyi Zhang, Moustapha Cisse, Yann N Dauphin, and David Lopez-Paz. mixup: Beyond empirical risk minimization. In *International Conference on Learning Representations*, 2018. 6

- [59] Jingzhao Zhang, Sai Praneeth Karimireddy, Andreas Veit, Seungyeon Kim, Sashank Reddi, Sanjiv Kumar, and Suvrit Sra. Why are adaptive methods good for attention models? *Advances in Neural Information Processing Systems*, 33:15383–15393, 2020. [1](#)
- [60] Zhun Zhong, Liang Zheng, Guoliang Kang, Shaozi Li, and Yi Yang. Random erasing data augmentation. In *Proceedings of the AAAI conference on artificial intelligence*, pages 13001–13008, 2020. [6](#)

Memory-Efficient 4-bit Preconditioned Stochastic Optimization

Supplementary Material

A. Practical 32-bit Shampoo

In this section, we provide the practical 32-bit Shampoo introduced in Sec. 3.1 and summarize it in Algorithm 2.

Algorithm 2 Practical 32-bit Shampoo

Input: initial weight $W_0 \in \mathbb{R}^{m \times n}$, initial preconditioning matrices $L_0 = \epsilon I_m$, $R_0 = \epsilon I_n$, $\hat{L}_0 = I_m$, $\hat{R}_0 = I_n$. Total update steps T , interval of updating preconditioners T_1 and T_2 , momentum parameter $\beta \in (0, 1)$. First-order optimizer \mathcal{F} with initial optimizer state s_0 .

Output: final weight W_T .

```

1: for  $k = 1, 2, \dots, T$  do
2:   Compute gradient  $G_k = \nabla \mathcal{L}_k(W_k)$ 
3:   if  $k \% T_1 \equiv 0$  then
4:      $\bar{L}_k = \beta L_{k-1} + (1 - \beta) G_k G_k^T$ 
5:      $\bar{R}_k = \beta R_{k-1} + (1 - \beta) G_k^T G_k$ 
6:   else
7:      $L_k = L_{k-1}$ ,  $R_k = R_{k-1}$ 
8:   end if
9:   if  $k \% T_2 \equiv 0$  then
10:    Compute maximum singular values  $\lambda_{\max}^L$  and
11:     $\lambda_{\max}^R$  of  $L_k$  and  $R_k$  by power iteration
12:    Compute  $\hat{L}_k = (L_k + \lambda_{\max}^L \epsilon I_m)^{-1/4}$  and  $\hat{R}_k =$ 
13:     $(R_k + \lambda_{\max}^R \epsilon I_n)^{-1/4}$  by Schur-Newton iteration
14:    else
15:       $\hat{L}_k = \hat{L}_{k-1}$ ;  $\hat{R}_k = \hat{R}_{k-1}$ 
16:    end if
17:     $\hat{G}_k = \hat{L}_k G_k \hat{R}_k$ ;  $\tilde{G}_k = (\|G_k\|_F / \|\hat{G}_k\|_F) \cdot \hat{G}_k$ 
18:     $W_k, s_k = \mathcal{F}(W_{k-1}, s_{k-1}, \tilde{G}_k)$ 
19:  end for

```

B. Proofs in Theoretical Analysis

We vectorize the update scheme as follows. Starting with the matrix form:

$$W_{k+1} = W_k - \eta_k \mathcal{D}(\hat{L}_k) G_k \mathcal{D}(\hat{R}_k),$$

and applying vectorization, we get:

$$\text{Vec}(W_{k+1}) = \text{Vec}(W_k) - \eta_k \left(\mathcal{D}(\hat{R}_k) \otimes \mathcal{D}(\hat{L}_k) \right) \text{Vec}(G_k).$$

Let $x_k := \text{Vec}(W_k)$, $g_k := \text{Vec}(G_k)$, and $H_k := \mathcal{D}(\hat{R}_k) \otimes \mathcal{D}(\hat{L}_k)$. we obtain the vectorized update scheme:

$$x_{k+1} = x_k - \eta_k H_k g_k, \quad (14)$$

where $\{H_k\}$ is a sequence of positive definite matrices.

Proposition B.1. For a b -bit quantization and any vector $x \in \mathbb{R}^d$, the following bound holds:

$$\|\mathcal{D}(\mathcal{Q}(x)) - x\|_\infty \leq \frac{\|x\|_\infty}{2^b}.$$

Proof. Consider any real number $a \in [-1, 1]$. In a b -bit quantization system, the interval between two consecutive representable values is given by $\Delta = \frac{2}{2^b} = \frac{1}{2^{b-1}}$. Thus, the quantization error satisfies $|\mathcal{Q}(a) - a| \leq \frac{\Delta}{2} = \frac{1}{2^b}$.

For any vector $x \in \mathbb{R}^d$, we apply the definitions of the operators \mathcal{Q} and \mathcal{D} as follows:

$$\begin{aligned} & \|\mathcal{D}(\mathcal{Q}(x)) - x\|_\infty \\ &= \left\| \|x\|_\infty \mathcal{Q}\left(\frac{x}{\|x\|_\infty}\right) - \|x\|_\infty \frac{x}{\|x\|_\infty} \right\|_\infty \\ &= \|x\|_\infty \left\| \mathcal{Q}\left(\frac{x}{\|x\|_\infty}\right) - \frac{x}{\|x\|_\infty} \right\|_\infty \\ &\leq \|x\|_\infty \cdot \frac{1}{2^b}. \end{aligned}$$

This completes the proof. \square

Proposition B.2. For the 4-bit Shampoo in Algorithm 1, if $\|(\mathcal{D}(\bar{C}_k^L) \mathcal{D}(\bar{C}_k^L)^T + \lambda_{\max}^L \epsilon I_m)^{-1/4}\|_{\text{off}, \max} \leq C_B$, then its preconditioners hold that

$$\mathcal{D}(\hat{L}_k) \succeq (\mathcal{D}(\bar{C}_k^L) \mathcal{D}(\bar{C}_k^L)^T + \lambda_{\max}^L \epsilon I_m)^{-1/4} - C_B n_k 2^{-b} I,$$

and

$$\mathcal{D}(\hat{L}_k) \preceq (\mathcal{D}(\bar{C}_k^L) \mathcal{D}(\bar{C}_k^L)^T + \lambda_{\max}^L \epsilon I_m)^{-1/4} + C_B n_k 2^{-b} I,$$

where $\|\cdot\|_{\text{off}, \max}$ is the maximal absolute value of all off-diagonal entries and n_k is the number of rows in W_k .

Proof. Unroll the update in Step 4, we have

$$\begin{aligned} & L_k \\ &= \beta L_{k-1} + (1 - \beta) G_k G_k^T \\ &= \beta (\beta L_{k-2} + (1 - \beta) G_{k-1} G_{k-1}^T) + (1 - \beta) G_k G_k^T \\ &= \beta^2 L_{k-2} + (1 - \beta) (G_k G_k^T + \beta G_{k-1} G_{k-1}^T) \\ &\quad \dots \\ &= \beta^k L_0 + (1 - \beta) \sum_{i=0}^{k-1} \beta^i G_{k-i} G_{k-i}^T \\ &= \beta^k L_0 + (1 - \beta) \sum_{i=0}^{k-1} \beta^i G_{k-i} G_{k-i}^T \\ &\succeq 0. \end{aligned}$$

Thus Step 11 is well-defined. Let $S_k = (\mathcal{D}(\bar{C}_k^L)\mathcal{D}(\bar{C}_k^L)^T + \lambda_{\max}^L \epsilon I_m)^{-1/4}$. Since only off-diagonal part is quantized, by Step 6, we have

$$\begin{aligned} \mathcal{D}(\hat{L}_k) &= \mathcal{D}(\mathcal{Q}(S_k)) \\ &= \mathcal{D}(\mathcal{Q}(S_k - \text{Diag}(S_k))) + \text{Diag}(S_k) \\ &= S_k - \text{Diag}(S_k) + \text{Diag}(S_k) + E_k \\ &= S_k + E_k, \end{aligned}$$

where $E_k = (S_k - \text{Diag}(S_k)) - \mathcal{D}(\mathcal{Q}(S_k - \text{Diag}(S_k)))$. By Proposition B.1, we have

$$\begin{aligned} \|E_k\|_{\max} &\leq \|S_k - \text{Diag}(S_k)\|_{\max} 2^{-b} \\ &\leq \left\| (\mathcal{D}(\bar{C}_k^L)\mathcal{D}(\bar{C}_k^L)^T + \lambda_{\max}^L \epsilon I_m)^{-1/4} \right\|_{\text{off}, \max} 2^{-b} \\ &\leq C_B 2^{-b}, \end{aligned}$$

where $\|\cdot\|_{\max}$ is the largest entry in magnitude of a matrix. Note that for any $x \in \mathbb{R}^d$,

$$|x^T E_k x| \leq C_B 2^{-b} (e^T |x|)^2 \leq C_B n_k 2^{-b} \|x\|^2,$$

where e is the vector with all elements being 1 and $|\cdot|$ is the operator of taking element-wise absolute value. Therefore, we have

$$\begin{aligned} \mathcal{D}(\hat{L}_k) &= (\mathcal{D}(\bar{C}_k^L)\mathcal{D}(\bar{C}_k^L)^T + \lambda_{\max}^L \epsilon I_m)^{-1/4} + E_k, \\ &\succeq (\mathcal{D}(\bar{C}_k^L)\mathcal{D}(\bar{C}_k^L)^T + \lambda_{\max}^L \epsilon I_m)^{-1/4} - C_B n_k 2^{-b} I. \end{aligned}$$

This completes the proof. \square

Given a matrix S , the proof of Proposition B.2 shows that if we quantize only the off-diagonal entries of S while keeping the diagonal entries, the quantization error E satisfies $\|E\|_{\infty} \leq 2^{-b} \|S\|_{\text{off}, \infty}$. However, if the entire S is quantized, the error becomes $2^{-b} \|S\|_{\infty}$. When the diagonal entries of S dominate each row, this selective quantization method can significantly reduce the quantization error.

B.1. Smooth Nonconvex Training Loss

Theorem B.1. *Suppose Assumption 5.1 holds. Let $\eta_k = \frac{c}{\sqrt{T+1}}$ with $c \in \left(0, \frac{\lambda_{H, \min}}{2L(1+\sigma^2)\lambda_{H, \max}^2}\right)$, then we have*

$$\mathbb{E} \left[\|\nabla f(\bar{x}_T)\|_2^2 \right] \leq \frac{2(f(x_0) - \bar{f}) + c^2 L \sigma^2 \lambda_{H, \max}^2}{c \lambda_{H, \min} \sqrt{T+1}},$$

where \bar{x}_T is randomly selected from $\{x_0, x_1, \dots, x_T\}$, and $\bar{f} = \min_{x \in \mathbb{R}^d} f(x)$.

Proof. Without any ambiguity, $\|\cdot\|$ denotes the L_2 norm of a vector or the spectral norm of a matrix. By Lipschitz

smoothness, we have

$$\begin{aligned} f(x_{k+1}) &\leq f(x_k) + \langle \nabla f(x_k), x_{k+1} - x_k \rangle + \frac{L}{2} \|x_{k+1} - x_k\|^2 \\ &= f(x_k) - \eta_k \langle \nabla f(x_k), H_k g_k \rangle + \frac{L \eta_k^2}{2} \|H_k g_k\|^2 \\ &\leq f(x_k) - \eta_k \langle \nabla f(x_k), H_k g_k \rangle + L \eta_k^2 \|H_k \nabla f(x_k)\|^2 \\ &\quad + L \eta_k^2 \|H_k (\nabla f(x_k) - g_k)\|^2. \end{aligned}$$

Rearranging the terms and taking expectations, we get

$$\begin{aligned} &\eta_k \mathbb{E} \left[\|\nabla f(x_k)\|_{H_k}^2 \right] \\ &\leq \mathbb{E}[f(x_k)] - \mathbb{E}[f(x_{k+1})] + L \eta_k^2 \mathbb{E} \left[\|H_k \nabla f(x_k)\|^2 \right] \\ &\quad + L \sigma^2 \eta_k^2 \|H_k\|^2 (1 + \|\nabla f(x_k)\|^2). \end{aligned}$$

By the choice of c , we have

$$\begin{aligned} &\frac{1}{2} \eta_k \|\nabla f(x_k)\|_{H_k}^2 \\ &\geq L \eta_k^2 \left(\|H_k \nabla f(x_k)\|^2 + \sigma^2 \|H_k\|^2 \|\nabla f(x_k)\|^2 \right), \end{aligned}$$

we have

$$\begin{aligned} &\frac{\sum_{k=0}^T \eta_k \mathbb{E} \left[\|\nabla f(x_k)\|_{H_k}^2 \right]}{2 \sum_{k=0}^T \eta_k} \\ &\leq \frac{f(x_0) - \bar{f} + L \sigma^2 \lambda_{H, \max}^2 \sum_{k=0}^T \eta_k^2}{\sum_{k=0}^T \eta_k}. \end{aligned}$$

In particular, when $\eta_k = \frac{c}{\sqrt{T+1}}$, we have

$$\mathbb{E} \left[\|\nabla f(\bar{x}_k)\|^2 \right] \leq \frac{2(f(x_0) - \bar{f}) + c^2 L \sigma^2 \lambda_{H, \max}^2}{c \lambda_{H, \min} \sqrt{T+1}}.$$

\square

B.2. Nonsmooth Nonconvex Training Loss

Conventional techniques in stochastic optimization for non-smooth nonconvex scenarios typically rely on the time-homogeneity of the associated dynamical system, as shown in [4, 13]. Given a locally Lipschitz function f , by Rademacher's theorem, f is differentiable almost everywhere. Thus, we have the following definition of subdifferential for a locally Lipschitz function.

Definition B.1. *The Clarke subdifferential or subgradient [9] is defined as*

$$\partial f(x) := \left\{ y : x_k \rightarrow x, \nabla f(x_k) \rightarrow y, \right. \\ \left. \text{where } f \text{ is differentiable at } x_k \right\}.$$

Definition B.2. A locally Lipschitz function is C^p -Whitney stratifiable [13], if the graph of f : $\text{graph}(f) := \{(x, t) : f(x) = t\}$ can be decomposed into finite C^p manifolds, called strata, satisfying

1. For any two strata \mathcal{M}_1 and \mathcal{M}_2 , the following implication holds:

$$\mathcal{M}_1 \cap \overline{\mathcal{M}_2} \neq \emptyset \implies \mathcal{M}_1 \subset \overline{\mathcal{M}_2}$$

2. For any sequence of points z_k in a stratum \mathcal{M}_1 converging to a point \bar{z} in a stratum \mathcal{M}_2 , if the corresponding normal vectors $v_k \in N_{\mathcal{M}_1}(z_k)$ converge to a vector v , then the inclusion $v \in N_{\mathcal{M}_2}(\bar{z})$ holds. Here $N_{\mathcal{M}_i}$ is the normal space of \mathcal{M}_i .

For example, the function $-|x|$ is a C^∞ -Whitney stratifiable function, with its graph decomposable into the sets $\{(0, 0)\}$, $\{(t, -t) : t > 0\}$ and $\{(t, t) : t < 0\}$.

Theorem B.2. Suppose Assumption 5.2 holds, and assume the sequence $\{x_k\}$ remains within a compact set. If the learning rate satisfies $\sum_{k=1}^\infty \eta_k = \infty$ and $\sum_{k=1}^\infty \eta_k^2 < \infty$, then

$$\lim_{k \rightarrow \infty} \text{dist}(x_k, \Omega) = 0,$$

where $\Omega := \{x : 0 \in \partial f(x)\}$ is the set of stationary points.

Proof. Define the interpolated process $x(t)$ for $\{x_k\}$ as follows:

$$x(t) := x_k + \frac{t - t_{k-1}}{\eta_k} (x_{k+1} - x_k), \quad \text{for } t \in [t_{k-1}, t_k),$$

where $t_k := \eta_1 + \dots + \eta_k$, $t_0 = 0$. Define $y(t) := H_k d_k$ for $t \in [t_{k-1}, t_k)$, where $d_k \in \partial f(x_k)$. Thus, both $x(t)$ and $y(t)$ are piecewise linear functions. We also define time-shifted versions $y^t(\cdot) := y(t + \cdot)$.

Let $x_t(\cdot)$ denote the solution to the following ODE:

$$\dot{x}_t(\tau) = -y(\tau), \quad x_t(t) = x(t), \quad \text{for any } \tau \geq t.$$

By Assumption 5.2, $\sup_k \|d_k\| \leq \ell$, so $\sup_{t \geq 0} \|y(t)\| \leq M\ell$. Therefore, the class of functions $\{x_t(\cdot) : t \geq 0\}$ is uniformly equicontinuous. Using the assumptions on $\{\xi_k\}$, the learning rate $\{\eta_k\}$, and the boundedness of H_k , it follows from [18, Lemma A.1] that for any $T > 0$,

$$\lim_{t \rightarrow \infty} \sup_{\tau \in [t, t+T]} \|x(\tau) - x_t(\tau)\| = 0.$$

Since $x(\cdot)$ is pointwise bounded, $x_t(\cdot)$ is also pointwise bounded. By the Arzelà-Ascoli theorem, the equicontinuity of $\{x_t(\cdot) : t \geq 0\}$ implies that it is relatively compact in the space of continuous functions, under the topology of uniform convergence over any compact set. The relative compactness of $\{y^t(\cdot)\}$ can be similarly verified; see [4, 6] for further details on related functional analysis concepts.

For any fixed $T > 0$, by the definition of $x_t(\cdot)$, we have

$$x_t(t+T) = x_t(t) - \int_0^T y^t(s) ds.$$

Now, select a subsequence $\{t_{k_j}\}$ such that the sequences $\{x_t(\cdot)\}$ and $\{y^t(\cdot)\}$ converge to $\bar{x}(\cdot)$ and $\bar{y}(\cdot)$, respectively, as $j \rightarrow \infty$. Letting $j \rightarrow \infty$, we obtain

$$\bar{x}(T) = \bar{x}(0) - \int_0^T \bar{y}(s) ds.$$

Next, we show that $\bar{y}(s) \in \bar{H}\partial f(\bar{x}(s))$. Note that

$$\begin{aligned} & \text{dist}(\bar{y}(s), \bar{H}\partial f(\bar{x}(s))) \\ & \leq \left\| \frac{1}{N} \sum_{j=1}^N y^{t_{k_j}}(s) - \bar{y}(s) \right\| \\ & \quad + \text{dist} \left(\frac{1}{N} \sum_{j=1}^N y^{t_{k_j}}(s), \bar{H}\partial f(\bar{x}(s)) \right) \\ & \leq \text{dist} \left(\frac{1}{N} \sum_{j=1}^N H_{\lambda(t_{k_j}+s)} d_{\lambda(t_{k_j}+s)}, \bar{H}\partial f(\bar{x}(s)) \right) + o(1), \end{aligned}$$

where $\lambda(t) = k$ such that $t_k < t \leq t_{k+1}$. Since $d_{\lambda(t_{k_j}+s)} \in \partial f(x_{\lambda(t_{k_j}+s)})$, by the outer-semicontinuity of ∂f , we have $\text{dist}(d_{\lambda(t_{k_j}+s)}, \partial f(\bar{x}(s))) \rightarrow 0$. Using Assumption 5.2c, we have

$$\begin{aligned} & \text{dist}(\bar{y}(s), \bar{H}\partial f(\bar{x}(s))) \\ & \leq \text{dist} \left(\frac{1}{N} \sum_{j=1}^N H_{\lambda(t_{k_j}+s)} d_{\lambda(t_{k_j}+s)}, \bar{H}\partial f(\bar{x}(s)) \right) + o(1) \\ & \rightarrow 0. \end{aligned}$$

Thus, we conclude the following:

$$\bar{x}(T) = \bar{x}(0) - \int_0^T \bar{y}(s) ds, \quad \text{and } \bar{y}(s) \in \bar{H}\partial f(\bar{x}(s)). \quad (15)$$

By [13, Theorem 3.2], any limit point of $\{x_k\}$ converges to the stable set of (15), namely, $\{x : 0 \in \bar{H}\partial f(x)\} = \{x : 0 \in \partial f(x)\} = \Omega$. This completes the proof. \square

C. Experimental Details

C.1. Training Hyperparameters

For the base first-order optimizers SGDM and AdamW used in Shampoo, we always maintain their optimizer states in 32-bit precision. For SGDM, we set the initial learning rate to 0.1, the momentum parameter to 0.9, and the weight decay coefficient to 5×10^{-4} for training CNNs on CIFAR-100 and Tiny-ImageNet, and 1×10^{-4} for training ResNet-50 on ImageNet. For AdamW, we set the initial learning

rate to 1×10^{-3} , the momentum parameters to $\beta_1 = 0.9$ and $\beta_2 = 0.999$, the small positive constant for the denominator to 1×10^{-8} , and the weight decay to 5×10^{-2} .

For quantization settings, we employ block-wise linear-2 quantization as introduced in Sec. 3.2, with a block size of $B \times B = 64 \times 64$. For tensors with fewer than 4096 elements, quantization is not applied.

For both 32-bit and 4-bit Shampoo, we set the small positive constant $\epsilon = 1 \times 10^{-6}$ and the preconditioner momentum parameter $\beta = 0.95$. For the momentum parameter of the error states, we set $\beta_e = 0.9$ for training CNNs and $\beta_e = 0.95$ for training ViTs. For update intervals, we use $T_1 = 100$ and $T_2 = 500$ for experiments on CIFAR-100 and Tiny-ImageNet, and $T_1 = 200$ and $T_2 = 1000$ for training ResNet-50 on ImageNet. Additionally, Shampoo applies preconditioning to blocks derived from large matrices, with the maximum order of the preconditioner set to 1200.

For image classification tasks, we use the traditional cross-entropy loss as the training loss. For the learning rate schedule, we employ cosine annealing with 5 epochs of linear warmup across all experiments.

The batch size is set to 128 for experiments on CIFAR-100 and Tiny-ImageNet, and to 256 for training ResNet-50 on ImageNet. For the total training epochs, we follow [23, 54] and train Shampoo with SGDM as the base optimizer for 200 epochs when training CNNs on CIFAR-100, while SGDM itself is trained for 300 epochs on CIFAR-100. For training CNNs on Tiny-ImageNet and ViTs on CIFAR-100 and Tiny-ImageNet, we follow [31, 33] and train Shampoo with the base optimizer for 100 epochs, and the base optimizer itself for 150 epochs. For training ResNet-50 on ImageNet, we train Shampoo with SGDM as the base optimizer for 100 epochs and SGDM for 120 epochs.

C.2. Memory Efficiency

In our experiments, we report the peak GPU memory usage instead of the memory used solely by the optimizers, as the peak GPU memory usage is the primary constraint when training large-scale models in practice and is therefore our main concern. Furthermore, from the total peak GPU memory usage, we can deduce the additional memory cost introduced by the preconditioners of Shampoo on top of the base optimizers.

For instance, when training ResNet-34 on CIFAR-100, the base optimizer SGDM incurs a peak memory usage of 1254.7 MB. The additional peak GPU memory usage caused by storing the 32-bit preconditioners of Shampoo $(L_k, R_k, L_k^{-1/4}, R_k^{-1/4})$ is calculated as the peak memory usage of 32-bit Shampoo minus 1254.7 MB, which equals 627.9 MB. With vanilla 4-bit quantization for the preconditioners, this additional memory usage drops to 86.3 MB, which is less than $1/7$ of the additional memory required by 32-bit Shampoo. Furthermore, when using 4-bit Sham-

poo with Cholesky quantization, the additional peak memory usage decreases further to 64.8 MB.

We now provide a brief analysis of why the increased peak memory usage of 4-bit Shampoo with Cholesky quantization (e.g., 64.8 MB) is approximately 75% of that of vanilla 4-bit Shampoo (e.g., 86.3 MB). Vanilla 4-bit Shampoo stores the 4-bit preconditioners $(L_k, R_k, L_k^{-1/4}, R_k^{-1/4})$, as introduced in Sec. 4.1, which consist of four full matrices of the same shape in 4-bit precision. In contrast, 4-bit Shampoo with Cholesky quantization stores $(C_k^L, C_k^R, L_k^{-1/4}, R_k^{-1/4})$ as described in Sec. 4.2, where C_k^L and C_k^R are the lower triangular Cholesky factors of L_k and R_k , respectively. The storage of C_k^L and C_k^R requires only half the space of L_k and R_k , leading to the total storage cost of the preconditioners for 4-bit Shampoo with Cholesky quantization being approximately 75% of that of vanilla 4-bit Shampoo.

For $L_k^{-1/4}$ and $R_k^{-1/4}$, Cholesky quantization is not applied, as they are used to precondition stochastic gradients at each iteration, as described in Algorithm 2 and Algorithm 1. Restoring them from their Cholesky factors at each iteration would be computationally expensive.